

A new setup for experiments with ultracold Dysprosium atoms

E. Lucioni^{1,3}, G. Masella¹, A. Fregosi², C. Gabbanini¹, S. Gozzini¹, A. Fioretti^{1,a}, L. Del Bino³, J. Catani^{3,4}, G. Modugno^{3,4}, and M. Inguscio³

¹ Istituto Nazionale di Ottica, CNR., S.S. “A. Gozzini” di Pisa, via Moruzzi 1, 56124 Pisa, Italy

² Dipartimento di Fisica, Università di Pisa, Largo B. Pontecorvo, 56127 Pisa, Italy

³ LENS and Dip. di Fisica e Astronomia, Università di Firenze, 50019 Sesto Fiorentino, Italy

⁴ Istituto Nazionale di Ottica, CNR, S.S. Sesto Fiorentino, 50019 Sesto Fiorentino, Italy

Abstract. In the domain of quantum degenerate atomic gases, much interest has been raised recently by the use of Lanthanide atoms with large magnetic moments, in particular Dysprosium and Erbium. These species have been successfully brought to quantum degeneracy and are now excellent candidates for quantum simulations of physical phenomena due to long-range interactions. In this short article, we report on the progresses in the construction of a new experiment on Bose-Einstein condensation of Dysprosium atoms. After completing the vacuum and the laser setups, a magneto-optical trap on the narrow 626 nm ¹⁶²Dy transition has been realized and characterized. The prospects for future experiments are briefly discussed.

Quantum degenerate dipolar systems are nowadays among the most interesting systems in quantum physics because they provide, to a very large extent, a clean and controlled experimental environment where long-range, anisotropic interactions can be finely tuned against short-range, isotropic ones. Although the dipolar interaction strength is much lower than that achievable in molecular systems, atomic samples are suitable to study a variety of phenomena thanks to the absence of large inelastic losses and to the immediacy of application of well-developed experimental techniques. Dipolar interactions in ultracold atoms, according to theoretical predictions [1,2,3], give rise to a wealth of peculiar quantum phenomena and exotic quantum phases, encompassing super-solids, quasi-crystals, frustrated crystals and self-assembled structures. These phenomena are due to the combination of the long-ranged and anisotropic nature of such interactions. Dipolar gases in optical lattices may widen the existing possibilities for the quantum simulation of condensed matter-like physics [4,5].

Among open-shell Lanthanides having the largest magnetic interaction, quantum degeneracy has been recently attained for Dysprosium [6,7] and Erbium [8,9], both nicely providing bosonic and fermionic isotopes in large natural abundance. These systems have shown a very rich collisional dynamics [10,11,12] due to their large spin and orbital angular momentum and, most of all, spectacular phase transitions [13,14]

^a e-mail: andrea.fioretti@ino.it

obtained by fine Feshbach tuning of the contact interaction with respect to the dipolar one. Finally, a first quantum simulation of the extended Hubbard model has been realized with a dipolar condensate in an optical lattice [15].

The starting point and working horse of all systems leading to quantum degeneracy in dilute gases is a magneto-optical trap (MOT). In open-shell Lanthanide atoms, given the complex electronic structure, it was far from being obvious that the MOT scheme would work but it has been successfully demonstrated initially with Erbium atoms [16]. The presence of several possible cycling transitions with different linewidths [16,17,18,19] offers the possibility of tailoring the cooling force and the final temperature in order to optimize the subsequent trapping in optical traps and evaporative cooling to quantum degeneracy.

We report here on the realization of a magneto-optical trap for ^{162}Dy atoms on the intermediate linewidth transition at 626 nm. We briefly describe our experimental setup and the characterization of the loading and trapping processes. Our results confirm those of a recent extended study of a Dy MOT [20] and represent a nice starting point for evaporative cooling to quantum degeneracy.

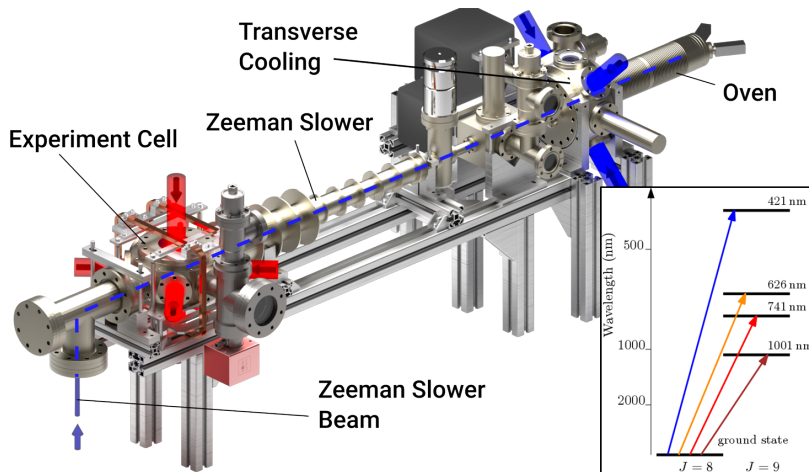


Fig. 1. Sketch of the experimental apparatus. Laser beams are indicated by blue (421 nm) and red (626 nm) arrows. In the inset, the $J \rightarrow J + 1$ transitions from Dy ground state are shown. The two transitions at 421 nm and 626 nm are used for slowing and trapping, respectively.

Disprosium melts at 1407°C and therefore a high temperature oven is necessary to obtain a reasonable vapour pressure, thus requiring substantial laser slowing in a Zeeman Slower (ZS). The experimental apparatus, shown in Fig. 1 along with Dy relevant electronic transitions, is made up of three main sections. In the first section, evacuated by a 201/s ion pump (Varian VacIon), an atomic beam is sourced from an effusive cell heated up to 1200°C . In order to exit the cell, the Dy atoms pass through a 3 cm-long collimation tube with a diameter of 4 mm. In this way forward emission is enhanced by reducing by a factor 10 the atomic beam divergence and a longer lifetime of solid Dysprosium in the crucible is guaranteed. A short stainless steel tube (4 cm diameter) after the cell is nevertheless used to prevent Dy atoms to stick on the side windows. The atomic beam is further collimated by a transverse cooling stage performed on the strongest transition at 421 nm (linewidth $\Gamma_{421} = 2\pi \times 32.2\text{ MHz}$). Transverse cooling beams are elliptically shaped (3.5 mm and 8 mm vertical and horizontal waists), light is red detuned by $0.3\Gamma_{421}$ from the atomic

transition and its intensity is higher than the saturation intensity ($I_{421} = 3 \times I_{\text{sat}}^{421}$ where $I_{\text{sat}}^{421} = 56.5 \text{ mW/cm}^2$) for a total power of 75 mW in the beams. We do not observe a saturation of the transverse cooling effect with the power and we suppose that a higher power would further increase the MOT loading efficiency.

A differential pumping stage separates the first section of the apparatus from the second one. This is composed of two narrow tubes (each 5 mm diameter and 81 mm length) pumped in between by another 20 l/s ion pump (Varian VacIon). Together with the ZS tube, they allow a differential vacuum between the transverse cooling cell and the science cell larger than three orders of magnitude. In this section the fraction of the atomic beam with velocity lower than about 550 m/s is slowed down to a final velocity of a few meters per second in a 52 cm long spin-flip Zeeman slower operating on the strong 421 nm transition as well. The ZS beam has a power of 150 mW, is red detuned by $27\Gamma_{421}$ ($2\pi \times 1.05 \text{ GHz}$) from the atomic transition, enters the ZS through an aluminum mirror positioned inside the vacuum apparatus at 45° [8] in order to avoid Dy coating on the window, and is focused of the effusive cell aperture to better match the atomic beam shape.

The third section consists of a stainless steel octagonal chamber where atoms from the slowed beam are captured in a magneto-optical trap (MOT) operating on the narrower atomic transition at 626 nm with a linewidth $\Gamma_{626} = 2\pi \times 136 \text{ kHz}$. The trapping beams have large waists (1.2-1.8 cm) and peak intensities of about $I_{626} = 120 \times I_{\text{sat}}^{626}$ where $I_{\text{sat}}^{626} = 72 \mu\text{W/cm}^2$) for a total power of 140 mW in the six beams, and a detuning Δ in the 1-6 MHz range. The magnetic field gradient is about 1.4 G/cm along the strong axis. This final section is evacuated by a NEX Torr D 100-5 hybrid pump (100 l/s getter + 6 l/s ion pump). This choice has the advantage of providing large pumping speed with reduced magnetic fields near the atoms.

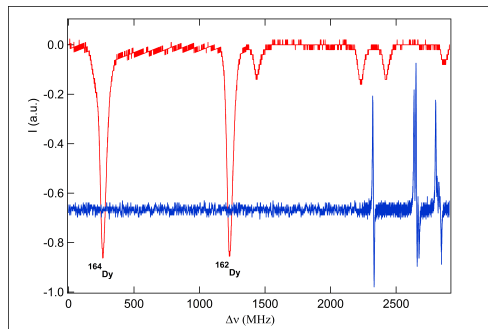


Fig. 2. Fluorescence spectrum (upper red curve) of the Dy atomic beam and error signal (lower blue curve) of the saturated absorption of Iodine as a function of the laser frequency near 626 nm. The largest peaks from the left come from the two bosonic species ^{164}Dy and ^{162}Dy , while the smaller ones belong to the fermions. We lock the laser to the left-most line of Iodine in the figure.

In order to generate light at 421 nm we frequency-double the light emitted from a Ti:Sa laser (SolsTiS by M Squared, 3W output at 800 nm) in a bow-tie cavity containing a LBO crystal ($3 \times 3 \times 15 \text{ mm}^3$, 27.8° angle, temperature 20°C , ideal beam waist $16 \mu\text{m}$). We can produce up to 1.6 W of blue light with a conversion efficiency larger than 50% [21]. The blue light is locked to the atomic transition by performing saturated absorption spectroscopy in a see-through hollow-cathode lamp by Heraeus (buffer gas pressure 5 torr). Although the residual laser linewidth is estimated to be well below 1 MHz, the accuracy of the lock is of the order of a

few MHz. Light at 626 nm is generated by a commercial laser system (TA-SHG pro by Toptica, 1 W at 626 nm, linewidth 20 kHz in $5 \mu\text{s}$). We lock the laser light to a Iodine transition using saturated absorption spectroscopy in a I_2 cell. The frequency gap between the locking point and the atomic transition (about 1 GHz for ^{162}Dy) is bridged with a sequence of AOMs. The residual laser linewidth is a few tens of kHz. Fig. 2 shows the relative position of the Dy and Iodine absorption lines. This lock on a Iodine line represents a cost-effective alternative to the lock on an Ultra Low Expansion cavity. Unfortunately, due to relative positions of Dysprosium and Iodine lines and to available AOMs, it gives access only to one of the two most abundant boson isotopes, i.e. ^{162}Dy . The laser light is conveyed to the different parts of the apparatus by single-mode, polarization-maintaining optical fibers.

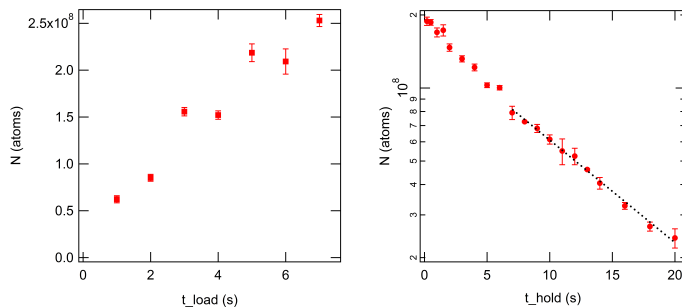


Fig. 3. (left part) Number of atoms in the MOT as a function of loading time; (right part) Number of remaining atoms in the MOT as function of the holding time; the line is a fit with a single exponential (see text). In both cases $\Delta = -35\Gamma$ and total laser power on the ZS is 130 mW.

In the following, the measurements performed in order to optimize and characterize the MOT loading are reported. Absorption imaging with resonant light at 421 nm along two orthogonal directions allows to extract the MOT dimensions and trapped atom number. A compression phase lasting 40 ms at reduced laser detuning ($\Delta_r = -10\Gamma_{421}$) and intensity ($I_r = 0.4I$), is performed after the MOT phase, prior to imaging, in order to increase the density and decrease the temperature.

The narrow linewidth of the MOT transition allows, in our experimental conditions, a very low capture velocity of about 5 m/s, as estimated from numerical simulations. In order to increase it, we have artificially increased the linewidth of the trapping laser during the loading phase by applying a frequency modulation at a rate of 136 kHz and amplitudes up to 2.0 MHz, as performed in Ref. [20]. This results in up to a factor 3 increase in the number of trapped atoms. The number of atoms as a function of the loading time by the ZS and of the holding time in the MOT are shown in Fig. 3. The atom capture rate at early times is $4.6 \times 10^7 \text{ s}^{-1}$ and the MOT atom number saturates after about 10 s. Typical densities, after the compression phase, are of the order of 10^{11} cm^{-3} . We notice that the decay curve can be nicely fitted with a single exponential (decay time $\tau = 10.3 \text{ s}$) only at long times, meaning that in our conditions the MOT density and the total loss rate are already affected by 2-body collisions. The temperature of the trapped atoms has been measured by absorption imaging after switching-off the MOT and letting the cloud expand freely for up to 30 ms, obtaining temperatures of about $20 \mu\text{K}$.

A study of the number of trapped atoms as a function of MOT laser detuning and modulation band-width is shown in Fig. 4. The observed trend is consistent with that observed in similar setups [18,19,20], i.e. optimum operating conditions

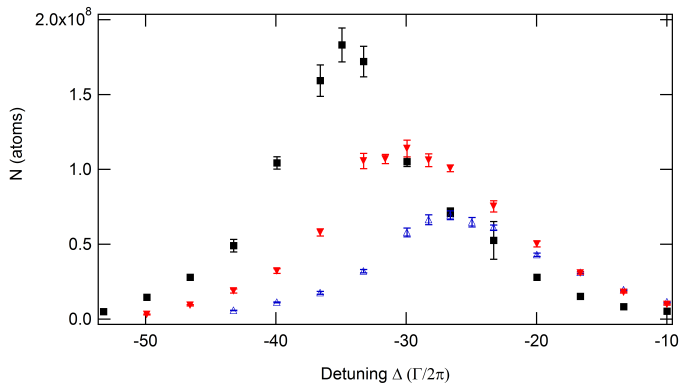


Fig. 4. Number of atoms in the MOT as function of the detuning in the loading phase respectively with: (full squares) 2.0 MHz laser linewidth, (full triangles) 1.1 MHz laser linewidth, (empty triangles) un-modulated laser, linewidth of a few tens kHz.

at large detuning values. This feature can be ascribed to the detuning-dependent gravitational sag of the MOT, larger than 1 cm for large detunings, which “protects” the MOT against losses due to the ZS light during loading. We observed that the trapped sample becomes more and more spin-polarized as the detuning is increased, due to the combined action of the gravitational sag and optical pumping. This is a particularly useful feature, studied in detail in Ref. [20], almost unique to this type of MOTs. We observed that spin-polarization can be reduced or lost during the compression phase if a small detunings or large intensities are employed. As an example, the data in Fig. 3 are not completely polarized.

In conclusion, we are able to trap in our setup over 2×10^8 ^{162}Dy atoms at temperatures as low as $20 \mu\text{K}$. This is a very good starting point for the subsequent evaporative cooling phase to quantum degeneracy. To this aim we have already included in our science cell a high-finesse in-vacuum Fabry-Perot cavity to realize a large-waist, standing-wave optical trap with a low power Nd-YAG laser. A similar scheme has been already employed for Li and Yb atoms [22,23]. This method allows to realize a deep optical trap with a large volume, healing the problem of the relatively low dipole polarizability of Dy atoms at $1 \mu\text{m}$ wavelength [20] and enhancing the capture of atoms from the MOT. After an initial evaporation stage, the atoms will be transferred to a standard crossed-beams optical trap and cooled evaporatively to quantum degeneracy. We plan to perform a first generation of experiments in the steel chamber, which provides sufficient optical access to realize optical lattices and other types of optical potentials (i.e. disorder or time-dependent potentials). For future experiments in well-controlled magnetic fields and with high-resolution imaging we plan to use a second glass chamber.

A first direction we plan to explore is that of low dimensional systems in ordered and disordered optical lattices. Working with short-wavelength lattices it is possible to enhance the effects of the dipolar interaction over the contact interaction [15]. In such regime, there are elusive and exotic quantum phases that could be addressed experimentally, such as supersolidity [24], crystallization [25] and many-body localization [26].

We thank M. Tagliaferri, M. Voliani, F. Pardini, A. Barbini, R. Ballerini, A. Hajeb, M. De Pas, M. Giuntini and M. Archimi for technical assistance during the construction of the apparatus, F. Ferlaino, G. Roati and D. Giulietti for interesting discussions, L. Fallani for providing the ZS and MOT simulation programs, and L.A. Gizzi for continuous support. This work was supported also by the ERC (Grants 203479 -

QUPOL and No. 247371 - DISQUA), by the EC - H2020 research and innovation programme (Grant No. 641122 - QUIC).

References

1. T. Lahaye *et al.*, Rep. Prog. Phys. **72**, (2009) 126401
2. C. Trefzger *et al.*, J. Phys. B **44**, (2011) 193001
3. M. Baranov, Chem. Rev. **112**, (2012) 5012
4. M. Lewenstein *et al.*, Adv. Phys. **56**, (2007) 243
5. I. Bloch *et al.*, Rev. Mod. Phys. **80**, (2008) 885
6. M. Lu, *et al.*, Phys. Rev. Lett. **107**, (2011) 190401
7. M. Lu, *et al.*, Phys. Rev. Lett. **108**, (2012) 215301
8. K. Aikawa, *et al.*, Phys. Rev. Lett. **108**, (2012) 210401
9. K. Aikawa, *et al.*, Phys. Rev. Lett. **112**, (2014) 010404
10. K. Baumann, *et al.*, Phys. Rev. A **89**, (2014) 020701(R)
11. T. Maier, *et al.*, Phys. Rev. A **92**, (2015) 060702(R)
12. T. Maier, *et al.*, Phys. Rev. X **5**, (2015) 041029
13. H. Kadau, *et al.*, Nature **530**, (2016) 194
14. L. Chomaz, *et al.*, Phys. Rev. X **6**, (2016) 041039
15. S. Baier, *et al.*, Science **352**, (2016) 201
16. A.J. Berglund, *et al.*, Phys. Rev. Lett. **100**, (2008) 113002
17. M. Lu, *et al.*, Phys. Rev. Lett. **104**, (2010) 063001
18. A. Frisch, *et al.*, Phys. Rev. A **85**, (2012) 051401(R)
19. T. Maier, *et al.*, Opt. Lett. **39**, (2014) 3138
20. D. Dreon, *et al.*, arXiv:1610.02284v1 [cond-mat.quant-gas]
21. L. Del Bino, Master Thesis, Univ. Firenze, 2015,
<http://quantumgases.lens.unifi.it/publications/theses>
22. B. Zimmermann, *et al.*, New Jour. Phys. **13**, (2011), 043007
23. G. Pagano, *et al.*, Nat. Phys. **10**, (2014) 198201
24. K. Goral *et al.*, Phys. Rev. Lett. **88**, (2002), 170406
25. S. Gopalakrishnan *et al.*, Phys. Rev. Lett. **111**, (2013), 185304
26. N. Y. Yao *et al.*, Phys. Rev. Lett. **113**, (2014), 243002